

Neutron-scattering and susceptibility study of spin chains and spin ladders in $(\text{Sr}_{0.8}\text{Ca}_{0.2})_{14}\text{Cu}_{24}\text{O}_{41}$

R. S. Eccleston

ISIS Facility, Rutherford Appleton Laboratory, Chilton, Didcot, Oxfordshire OX10 0QX, United Kingdom

M. Azuma and M. Takano

Institute for Chemical Research, Kyoto University, Uji, Kyoto-fu 611, Japan

(Received 4 March 1996)

We have performed inelastic-neutron-scattering and dc susceptibility measurements on a polycrystalline sample of $(\text{Sr}_{0.8}\text{Ca}_{0.2})_{14}\text{Cu}_{24}\text{O}_{41}$, which has a complex crystal structure comprising alternating layers containing isolated CuO_2 chains and Cu_2O_3 two-legged ladders. The observed excitation spectrum is consistent with a spin gap for the ladder of 35 meV. At lower energy transfers we have observed a broad, nondispersive, feature centered on 10 meV that corresponds to singlet-triplet excitations in the CuO_2 chains. We see some evidence in our susceptibility and neutron-scattering measurements to suggest that portions of the CuO_2 chains are dimerized, or broken up into larger finite chains by nonmagnetic CuO_2 units. [S0163-1829(96)51822-9]

There has recently been much interest in the excitation spectrum of low-dimensional Heisenberg magnetic systems, much of it motivated by Haldane's prediction¹ that integer and half integer spin chains will exhibit qualitatively different excitation spectra with integer-spin chains displaying a spin gap and half-integer spin chains remaining gapless. This conjecture has been tested on several systems using neutron scattering and it is now generally held to be true. The close relationship between two-dimensional magnetism and high-temperature superconductivity has also done much to stimulate research in this field.

The Heisenberg spin ladders, which for $S=1/2$ are comprised of $S=1/2$ chains coupled antiferromagnetically to produce a ladder structure, provides an intermediate between one- and two-dimensional spin systems. They are described by the Hamiltonian

$$H = J_{\parallel} \sum_{\uparrow\downarrow} \mathbf{S}_i \cdot \mathbf{S}_j + J_{\perp} \sum_{\downarrow} \mathbf{S}_i \cdot \mathbf{S}_j,$$

where J_{\parallel} and J_{\perp} are interactions along the chains, and along the rungs of the ladder respectively. Both theoretical and experimental studies² have shown spin ladders to display several interesting physical properties of their own and it has been suggested that they may become superconductors upon hole doping.³ Ladders made up of an even number of chains are predicted to display a spin gap,⁴ whereas those with an odd number of chains are predicted to be gapless.⁵⁻⁷ Examples of Heisenberg spin ladders are rare in nature. The two-legged ladder $(\text{VO})_2\text{P}_2\text{O}_7$ has been studied by neutron scattering⁸ and a spin gap of 3.7 meV has been observed in excellent agreement with predictions. A spin gap has also been observed by magnetic susceptibility measurements,⁹ and very recently by neutron scattering,¹⁰ in the two-legged ladder compound SrCu_2O_3 . Cuprate materials such as the $\text{Sr}_{n-1}\text{Cu}_{n+1}\text{O}_{2n}$ series¹¹ and $\text{LaCuO}_{2.5}$ (Ref. 12) have attracted considerable interest because of the opportunity to

study the evolution of the magnetic properties with the width of the ladders and the potential for hole doping in the later material.

The crystal structure of $\text{Sr}_{14}\text{Cu}_{24}\text{O}_{41}$ (Ref. 13) comprises layers containing the same ladder structure exhibited by SrCu_2O_3 alternating with layers made up of CuO_2 chains. A plain view of the two layers is shown in Fig. 1. The ladders are considered to be isolated magnetically because the links between the two ladders are via 90° Cu-O-Cu bonds, which produces a weak ferromagnetic exchange coupling leading to frustration. Intraladder links, on the other hand, are via 180° Cu-O-Cu bonds which provides strong antiferromagnetic coupling between the Cu^{2+} ions. Recent NMR measurements¹⁴ provide evidence for a spin wave gap of 63 meV for the spin ladder in $(\text{Sr}_{0.4}\text{Ca}_{0.6})_{14}\text{Cu}_{24}\text{O}_{41}$. Within the chain the Cu^{2+} - Cu^{2+} link is via nearly 90° Cu-O-Cu bonds yielding a weak ferromagnetic coupling. In the case of $\text{Sr}_{14}\text{Cu}_{24}\text{O}_{41}$, bond-valence-sum calculations¹⁵ give an average Cu valence in the CuO_2 chains of $\text{Cu}^{2.4+}$. The holes are apparently localized to the CuO_2 chains, and the cou-

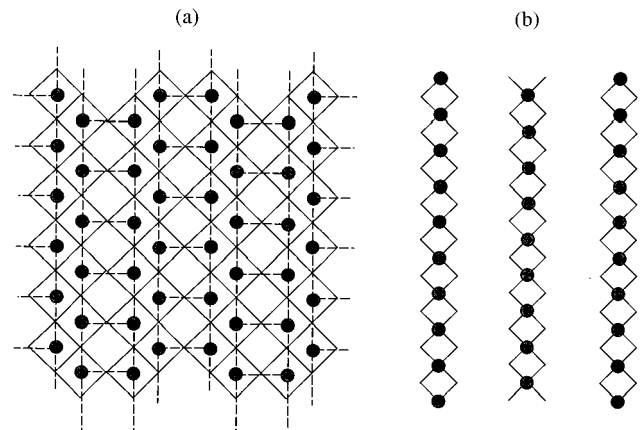


FIG. 1. The two layers of the $\text{Sr}_{14}\text{Cu}_{24}\text{O}_{41}$ structure, comprising isolated chains (b) and two-legged ladders (a).

pling within the chains is antiferromagnetic rather than ferromagnetic. Susceptibility measurements¹⁶ show that each hole in a CuO_2 chain causes approximately one CuO_2 unit to become nonmagnetic by creating a Zhang-Rice singlet.¹⁷ These data and electron spin resonance¹⁸ measurements show strong evidence for a singlet triplet gap for the chain of approximately 10 meV which probably arises from dimerization of the chain. This dimerization may arise as a result of nonmagnetic CuO_2 ions breaking up the chain, although other mechanisms have been suggested¹⁸ including structural distortion, as occurs in spin Peierls compounds, and spontaneous dimerization of the chain as a result of competition between nearest-neighbor and next-nearest-neighbor interactions as predicted by Haldane.¹⁹ It is not clear why the coupling in the chains is antiferromagnetic rather than ferromagnetic. Ca and Sr are isovalent, however, replacing Sr with Ca increases the conductivity of $(\text{Sr}_{1-x}\text{Ca}_x)_{14}\text{Cu}_{24}\text{O}_{41}$ until there is an insulator-metal transition when approximately half the Sr has been replaced by Ca, possibly due to a small transfer of holes from the CuO_2 chains to the Cu_2O_3 ladders.¹⁵

In this paper, we report neutron-scattering and dc magnetic susceptibility results from a polycrystalline sample of $(\text{Sr}_{0.8}\text{Ca}_{0.2})_{14}\text{Cu}_{24}\text{O}_{41}$. We have observed scattering consistent with a gap of 35 meV for the spin ladder and a broad feature at 10 meV which is consistent with the breakup of the CuO_2 chains into finite lengths due to the presence of nonmagnetic ions in the chain. Our neutron-scattering data suggest that portions of the CuO_2 chain are dimerized and the CuO_2 chain contribution to our susceptibility data can be described by a dimer-chain model, in which different interactions J_1 and J_2 alternate along the chain as described by the Hamiltonian

$$H = \sum_i \{J_1 \mathbf{S}_{2i} \cdot \mathbf{S}_{2i+1} + J_2 \mathbf{S}_{2i+1} \cdot \mathbf{S}_{2i+2}\}.$$

In the case of a polycrystalline sample the scattering law for a one-dimensional system is the powder average of the dynamic spin-spin correlation function²⁰

$S(Q, \omega)$

$$= \frac{1}{4\pi Q^2} T(\omega) |F(Q)|^2 \int_{\mathbf{q}=\mathbf{q}_{\parallel}+\mathbf{q}_{\perp}, |\mathbf{q}|=Q} S(\mathbf{q}_{\parallel}, \mathbf{q}_{\perp}, \omega) d\mathbf{q}, \quad (1)$$

where $F(Q)$ is the ionic form factor, \mathbf{q}_{\parallel} and \mathbf{q}_{\perp} are the parallel and perpendicular projections of the total momentum transfer \mathbf{q} relative to the chain axis, and $T(\omega)$ is the temperature factor

$$T(\omega) = \left[1 - \exp\left(\frac{-\hbar\omega}{k_B T}\right) \right]^{-1}.$$

Clearly for any given Q , all values of $|\mathbf{q}_{\parallel}| \leq Q$ will contribute to the scattered spectrum. For dispersive excitations $S(Q, \omega)$ is proportional to the density of states of the dispersion, consequently, where there is a singularity in the density of states, such as at a band minima, one expects a peak in the scattered intensity. For a mode with a minima at $|\mathbf{q}_{\parallel}| = q_1$ and energy transfer $\omega = E_g$ for example, one would expect no

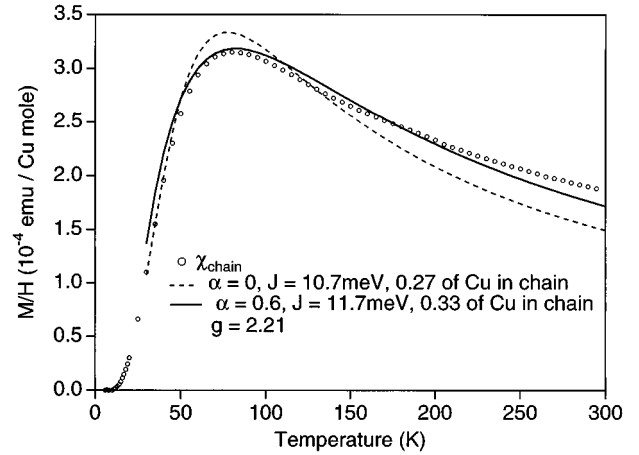


FIG. 2. The chain component of the susceptibility (points) with a fit to the dimer-chain model.

contribution to the scattering for $\omega = E_g$, $Q < q_1$, but a peak in the scattering at $\omega = E_g$, $Q = q_1$ which would persist to higher Q with the intensity modulated by Q and the form factor following Eq. (1).

The sample was prepared by the standard solid-state reaction from a mixture of SrCO_3 , CaCO_3 , and CuO in flowing oxygen. The dc susceptibility measurement described here was performed with a superconducting quantum interference device magnetometer (Quantum Design, MPMS2) in an external field of 10^4 Oe on cooling. A Curie component corresponding to 3.4% of the Cu spins was subtracted and the contribution of the Cu_2O_3 planes has been estimated assuming that their magnetic behavior is the same in this material as it is in SrCu_2O_3 . The remaining susceptibility arises from the CuO_2 chains. Figure 2 shows the chain component of the susceptibility and a fit using the dimer-chain model,²¹ which yields a value of $\alpha (= J_2/J_1) = 0.6$ and $J_1 = 11.7$ meV, giving a spin gap of 6.5 meV.²² This fit, however, only accounts for approximately one third of the Cu spins in the CuO_2 chains in agreement with previous susceptibility measurements.¹⁶

The neutron-scattering data described hereafter were collected on the HET and MARI direct geometry chopper spectrometers at the ISIS pulsed neutron facility at the Rutherford Appleton Laboratory. In both cases the white pulsed neutron beam is monochromated by a Fermi chopper which rotates at frequencies of up to 600 Hz and is phased to the neutron pulse. The energy transferred to the sample is then calculated from the time of flight of the scattered neutron. MARI offers continuous detector coverage over an angular range of 3.4° to 134° with a sample to detector distance of 4 m. HET is optimized for scattering at low momentum transfers over a wide energy range, with banks of detectors at 4 and 2.5 m covering the angular ranges 2.6° to 7° and 9° to 29° degrees respectively. Two further detector banks at 4 and 2.5 m at mean scattering angles of 115° and 133° are used to collect high Q data which are used for the estimation of the nonmagnetic background signal.

For the HET measurements the sample was wrapped in a flat Al foil sachet and attached to the cold finger of a closed cycle refrigerator (CCR). However, for the MARI experiment an annular sample geometry was used with the sample

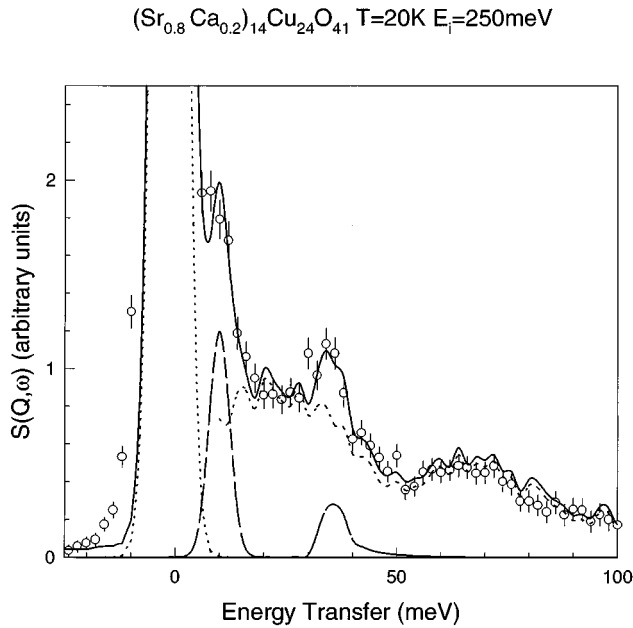


FIG. 3. Scattering from $(\text{Sr}_{0.8}\text{Ca}_{0.2})_{14}\text{Cu}_{24}\text{O}_{41}$ with an incident energy of 250 meV at a mean scattering angle (ϕ) of 4.7° at 20 K on HET. The solid line is the result of the fit described in the text. The magnetic component of the fit is represented by long dashed lines, the nuclear and single and multiphonon scattering is represented by short dashed lines.

mounted in an Al sample can filled with He exchange gas, before being attached to the CCR.

From the susceptibility data of Azuma *et al.*⁹ we anticipate a gap for the ladder of 36 meV at a momentum transfer $Q = 0.8 \text{ \AA}^{-1}$, because the Cu-O-Cu distance along the ladder is 3.94 \AA . This point falls outside the kinematic range of both instruments, however, by using an incident energy of 250 meV we were able to reduce the Q at an energy transfer of 35 meV to 0.93 \AA^{-1} . Figure 3 shows data collected on HET under these conditions. The points show the experimental points collected at a mean scattering angle of 4.7° . The solid line is the result of fitting a convolution of Eq. (1) with the instrumental resolution function to the data using the dispersion relation for a spin ladder with $J_{\parallel} = J_{\perp}$ predicted by Barnes and Riera.²³ The dashed line is an estimation of the single and multiphonon background from data collected in the high-angle detector banks, where the inelastic scattering is solely single and multiphonon in origin. Two scaling factors for the background were used as free parameters in the fit. A Gaussian was used to account for the magnetic intensity at energy transfers below 15 meV which could not be resolved from the elastic peak at this incident energy. This fit yields a value for the spin gap of $E_g = 34.9 \text{ meV}$ in excellent agreement with the value of 36 meV obtained by Azuma *et al.*⁹

Data collected on MARI with an incident energy of 20 meV are shown in Fig. 4. Once again the dashed line represents the nonmagnetic background signal which is determined from data collected at high scattering angles. The broad feature centered at 10 meV shows no dispersion with the intensity decreasing as expected from the Cu^{2+} form factor. Figure 5 shows the integrated intensity of the sharp

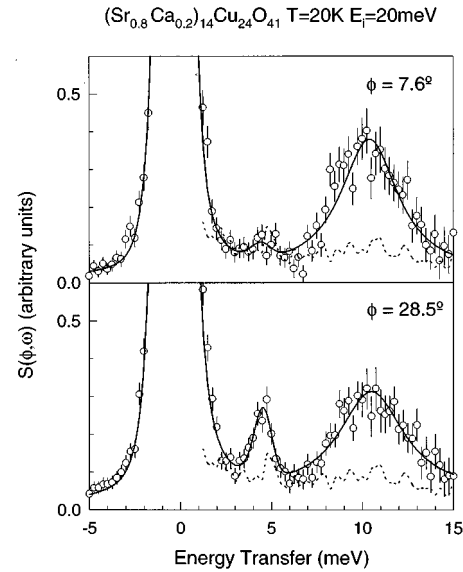


FIG. 4. Scattering from $(\text{Sr}_{0.8}\text{Ca}_{0.2})_{14}\text{Cu}_{24}\text{O}_{41}$ with an incident energy of 20 meV at mean scattering angles of $\phi = 7.6^\circ$ and $\phi = 28.5^\circ$ at 20 K on MARI. The solid lines represent a fit to the data as described in the text, the short dashed lines the phononic background estimated from data collected at high scattering angles.

peak at 4 meV as a function of Q with a fit to the dimer structure factor. Although the fit is not excellent, the oscillatory behavior characteristic of a dimer excitation is evident.

It seems clear that the CuO_2 chains contain CuO_2 units which are rendered nonmagnetic by the addition of a hole. The sharp peaks at 4 meV arises from dimers while the broad feature centered upon 10 meV may originate from longer finite chain lengths separated by nonmagnetic ions. The coexistence of dimers and longer finite chains explains the fact that the susceptibility data only accounts for one third of the copper spins in the chains. A chain of dimers separated by single nonmagnetic atoms would constitute a dimer chain, but it is not clear that any of the observed scattering arises from a dimer chain rather than isolated dimers. This infor-

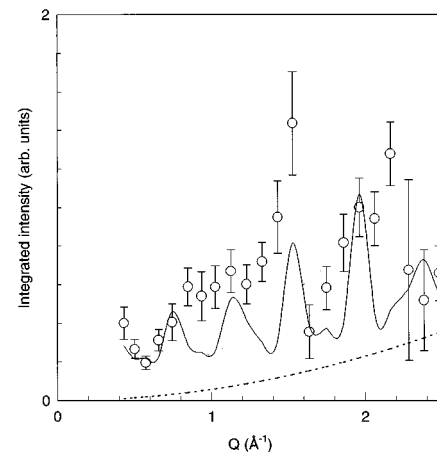


FIG. 5. Q dependence of the integrated intensity of the 4 meV peak. The dashed line represents an estimate of the nonmagnetic background scattering, and the solid line a fit to the data using the dimer structure factor.

mation will be best obtained by measuring these low-energy excitations in a single crystal where the dimer-chain dispersion could be measured directly. Since we have used a polycrystalline sample for these experiments we are not in a position to rule out interchain coupling and two-dimensional effects.

We have studied the excitation spectrum of $(\text{Sr}_{0.8}\text{Ca}_{0.2})_{14}\text{Cu}_{24}\text{O}_{41}$ by inelastic neutron scattering and have observed a spin gap for the Cu_2O_3 ladders of 35 meV. A broad nondispersive feature has been observed at 10 meV which may correspond to singlet-triplet excitations of finite chain lengths. A dimer excitation is observed at 4 meV. We plan to perform further experiments on other materials in the $(\text{La,Sr,Ca})_{14}\text{Cu}_{24}\text{O}_{41}$ family in order to study the effects of hole doping on the magnetic properties of the CuO_2 chains.

We anticipate that single crystals of sufficient volume for inelastic neutron scattering will soon be available allowing a more thorough investigation of the excitation spectrum of the ladder and of the CuO_2 chains.

We are grateful to Dr. Toby Perring, Dr. Hannu Mutka, and Dr. Eugene Goremychkin for many interesting discussions, Dr. Stephen Bennington for his assistance during the MARI experiment, and to members of the ISIS Operations Group for experimental support. This work is partly supported by a Grant in Aid for Scientific Research on Priority Area, "Anomalous metallic state near the Mott transition" of Ministry of Education, Science and Culture, Japan. We acknowledge the provision of neutron beamtime by the UK EPSRC.

-
- ¹F.D.M. Haldane, *Phys. Rev. Lett.* **50**, 1153 (1983).
²For a review see, E. Dagotto and T.M. Rice, *Science* **271**, 619 (1996).
³E. Dagotto, J. Riera, and D. Scalapino, *Phys. Rev. B* **45**, 5744 (1992).
⁴T. Barnes, E. Dagotto, J. Riera, and E.S. Swanson, *Phys. Rev. B* **47**, 3196 (1993).
⁵T.M. Rice, S. Gopalan, and M. Sigrist, *Europhys. Lett.* **23**, 445 (1993).
⁶S. Gopalan, T.M. Rice, and M. Sigrist, *Phys. Rev. B* **49**, 8901 (1994).
⁷S.R. White, R.M. Noack, and D.J. Scalapino, *Phys. Rev. Lett.* **73**, 886 (1994).
⁸R.S. Eccleston, T. Barnes, J. Brody, and J.W. Johnson, *Phys. Rev. Lett.* **73**, 2626 (1994).
⁹M. Azuma, Z. Hiroi, M. Takano, K. Ishida, and Y. Kitaoka, *Phys. Rev. Lett.* **73**, 3463 (1994).
¹⁰R.S. Eccleston, M. Azuma, and M. Takano (unpublished).
¹¹Z. Hiroi, M. Azuma, M. Takano, and Y. Bando, *J. Solid State Chem.* **95**, 230 (1991).
¹²Z. Hiroi and M. Takano, *Nature* **377**, 41 (1995).
¹³E.M. McCarron, M.A. Subramanian, J.C. Calabrese, and R.L. Harlow, *Mater. Res. Bull.* **23**, 1355 (1988).
¹⁴J. Akimitsu, M. Uehara, T. Nagata, S. Matsumoto, Y. Kitaoka, H. Takahashi, and N. Mōri (unpublished).
¹⁵M. Kato, K. Shiota, and Y. Koike (unpublished).
¹⁶S.A. Carter, R.J. Cava, B. Batlogg, J.J. Krajewski, W.F. Peck, Jr., and T.M. Rice (unpublished).
¹⁷F. Zhang and T.M. Rice, *Phys. Rev. B* **37**, 3759 (1988).
¹⁸M. Matsuda and K. Katsumata (unpublished).
¹⁹F.D.M. Haldane, *Phys. Rev. B* **25**, 4925 (1982).
²⁰H. Mutka, C. Payen, P. Molinie, J.L. Soubeyroux, P. Colombert, and A.D. Taylor, *Phys. Rev. Lett.* **67**, 497 (1991).
²¹J.W. Hall, W.E. Marsh, R.P. Weller, and W.E. Hatfield, *Inorg. Chem.* **20**, 1033 (1981); **20**, 1037 (1981).
²²J.C. Bonner and H.W.J. Blöte, *Phys. Rev. B* **25**, 6959 (1982).
²³T. Barnes and J. Riera, *Phys. Rev. B* **50**, 6817 (1994).